Journal of Machine Engineering, 2026, Vol. 26
ISSN 1895-7595 (Print) ISSN 2391-8071 (Online)

Received: *11 December 2025* /Accepted: *05 May 2026* / Published online: *20 May 2026*

machine learning, Johnson-Cook model,
invertible neural network,
parameter inverse identification

Mingfei MEI[1*], Tim REEBER[2],
Steffen EHNERT[2], Kung-Chiao WANG[2],
Kamil GÜZEL[2], Hans Christian MOEHRING[3]

INVERSE IDENTIFICATION OF JOHNSON-COOK PARAMETERS USING AN INVERTIBLE NEURAL NETWORK

The Johnson-Cook (J-C) model is a widely used constitutive model for describing the deformation and failure behaviour of metals under various strains, strain rates and temperatures. However, deviations often exist between simulated and experimental results, such as cutting forces, meaning that reliable cutting simulations require accurate material model parameters. The inverse identification of J-C parameters has therefore been an active research topic. Nevertheless, the inverse problem is inherently ambiguous, as different combinations of J-C parameters can produce similar cutting forces in simulations. This study aims to predict possible J-C parameter sets based on cutting and thrust forces obtained from a series of orthogonal cutting simulations based on AISI 1045 steel. An Invertible Neural Network (INN) is employed to inversely generate J-C parameter combinations, and real orthogonal cutting experiments are conducted to validate the reliability of the generated parameters. The results demonstrate that the INN can generate reliable and physically consistent J-C parameters.

1. INTRODUCTION

The Johnson-Cook (J-C) constitutive model is one of the most widely used material models to describe the material flow behaviour of metals under various strains, strain rates and temperatures [1]. It provides a simple analytical form that allows for efficient numerical implementation in finite element method (FEM), making it especially suitable for metal cutting and high strain rate deformation processes. Traditionally, J-C parameters are obtained through mechanical tests such as quasi-static tensile tests, Split-Hopkinson pressure bar experiments, and thermal softening tests [2, 3]. However, these methods are often time-consuming, expensive, and limited by experimental accessibility.

To overcome these limitations, many researchers have adopted FEM-based inverse identification strategies. In this approach, FEM simulations and experimental measurements are integrated to accelerate the parameter identification process. For instance, Aghdami et al.

[1] Machine design, Institute for Machine Tools, University of Stuttgart, Germany
[2] Process Monitoring and Control, Institute for Machine Tools, University of Stuttgart, Germany
[3] Institute for Machine Tools, University of Stuttgart, Germany
[*] E-mail: mingfei.mei@ifw.uni-stuttgart.de
https://doi.org/10.36897/jme/221466

employed a least-squares-based inverse analysis, in which the experimentally measured drawing forces were fitted to those obtained from FEM simulations, in order to inversely identify the most appropriate J-C parameters from 10100 copper and AA 1100 aluminum [4]. Similarly, in the work from Klocke et al., the strain hardening parameters A, B, and n from Inconel 718 and AISI 1045 were first determined from quasi-static compression tests via a least-squares fitting of the true stress-strain curves, while the strain-rate and thermal softening parameters C and m were optimized through a full factorial FEM-experiment interpolation [5]. Bäker adopted a descriptor-based inverse identification algorithm, in which the cutting force and shear angle served as observable proxies, and the J-C parameters were systematically tuned until the simulated responses matched the reference results within a small tolerance [6].

With the rapid progress of machine learning and deep learning, researchers have introduced data-driven approaches to accelerate the inverse identification of constitutive parameters. Jiang et al. proposed a genetic-algorithm-based inverse identification approach for the J-C constitutive model of 304 stainless steel. The J-C parameters were optimized using a genetic algorithm combined with least-squares fitness evaluation, where the deviation between simulated and experimental cutting forces served as the objective function [7]. Titu et al. developed a neural-network-based inverse modelling framework to estimate the five J-C material parameters and chip thickness for aluminum 6061-T6. Two neural network models were trained, namely: a forward model that mapped J-C parameters and chip thickness to the corresponding cutting responses, and a backward model that searched the input space of the forward network using to identify the set of J-C parameters and chip thickness [8]. However, it is important to note that the inverse identification of J-C parameters can be regarded as a problem of inferring hidden system variables (high dimension) from observable quantities (low dimension). In this context, the J-C parameters act as latent variables that encoded the underlying material behaviour, while the measurable outputs, such as cutting and thrust forces, represent only indirect expressions of these hidden physical properties. Therefore, the task of J-C parameter identification belongs to the broader class of ill-posed inverse problems, where multiple combinations of latent variables can reproduce the same set of observations.

In recent years, generative machine learning models have emerged as powerful tools for ill-posed inverse problems. Unlike traditional deterministic regressions that yield a single solution, generative models learn the underlying data manifold and enable stochastic sampling from a learned latent space, thus generating multiple feasible parameter combinations that reproduce the similar experimental observations [9]. Kumar et al. combined the genetic algorithm and Conditional Variational Autoencoder (CVAE) to address non-uniqueness in inverse photonic design. The CVAE learned the probabilistic mapping between layer thicknesses and optical spectra, while a genetic algorithm optimized latent variables to generate multiple valid designs [10]. Dan et al. proposed a generative machine learning model based on a Generative Adversarial Network (GAN) for efficient generation of new hypothetical inorganic materials [11]. Ardizzone et al. proposed an invertible neural network framework to address ill-posed inverse problems by learning the forward mapping from system parameters to observations. Once trained, the inverse network can recover the full posterior distribution of input parameters conditioned on a given measurement, allowing multiple valid solutions to be captured simultaneously [12].

The above studies highlight that generative models can effectively handle non-unique mappings and uncertainty in inverse problems. Building upon this concept, the present work employed a generative approach to predict the J-C parameters. An INN framework is adopted, where the inverse process is utilized to generate candidate J-C parameter sets, while the forward process is employed to predict cutting forces, thereby accelerating the overall evaluation process compared to FEM simulations. In addition, orthogonal cutting experiments are performed to validate the reliability and physical consistency of the generated parameters, demonstrating that the proposed INN framework can bridge the gap between simulation-based identification and experimental validation.

2. MATERIALS AND METHODS

2.1. DATASET

The constitutive model is a general formulation that characterizes the fundamental behaviour of materials under deformation. It establishes the relationships among thermomechanical parameters arising from the coupled effects of stress, strain, strain rate, and temperature during the deformation process [13]. In this study, the J-C constitutive model was employed to describe the flow stress-strain relationship of the material. The model is expressed as:

$$\sigma = (A + B\varepsilon^n)\left[1 + \mathrm{Cln}\left(\frac{\dot{\varepsilon}}{\dot{\varepsilon_0}}\right)\right]\left[1 - \left(\frac{T-T_r}{T_m-T_r}\right)^m\right] \tag{1}$$

where A is the initial yield stress (MPa), B is the strain hardening coefficient (MPa), C is the strain rate sensitivity, n is the strain hardening exponent, and m is the thermal softening exponent. σ denotes the flow stress (MPa), ε is the equivalent plastic strain, $\dot{\varepsilon}$ is the equivalent strain rate (s^{-1}), and $\dot{\varepsilon}_0$ is the reference strain rate for the material. T represents the deformation temperature $(^\circ\mathrm{C})$, T_m is the melting temperature $(^\circ\mathrm{C})$, and T_r is the room temperature $(^\circ\mathrm{C})$ [14].

In this study, the used dataset is provided by Reeber et al. [15], which includes cutting and thrust forces corresponding to different sets of J-C parameters obtained from 2D orthogonal cutting simulations. The dataset was generated using the commercial software for finite element analysis (FEA) Abaqus and the design procedures were discussed in [15]. In all simulation, the cutting speed is 100 m/min, the undeformed chip thickness is set to 0.1 mm, the width of cut is 0.25 mm. During dataset generation, only the J-C parameters were varied, while all other factors, such as boundary conditions, contact interactions, material properties, and cutting parameters, were kept constant. The dataset is based on the J-C parameters of AISI 1045 steel [16], and was further extended to cover a broader parameter range. Each J-C parameter was assigned four discrete levels (-40% 0% 40% 80%), resulting in 1024 (4^5) combinations. The dataset was shuffled and split into 80% for training and 20% for testing. Table 1 summarizes the statistical characteristics of the variables used in this study, including the mean, standard deviation (SD), and four discrete levels.

Table 1. Dataset overview

	Mean	SD	-40%	0%	+40%	+80%
A [MPa]	738.96	275.53	369.48	615.8	862.12	1108.44
B [MPa]	801.24	298.75	400.62	667.7	934.78	1201.86
c	0.0161	0.006	0.00804	0.0134	0.01876	0.02412
n	0.306	0.114	0.153	0.255	0.357	0.459
m	1.294	0.482	0.6468	1.078	1.5092	1.9404
F_c [N]	82.89	20.62	34.1924	73.7508	100.363	132.417
F_t [N]	36.77	8.55	20.3024	32.511	42.0484	55.6411

2.2. INVARIABLE NEURAL NETWORKS

Recent studies have shown that invertible neural networks (INNs) are capable of learning both forward and inverse mappings within a unified bijective architecture [12]. Once trained, the INNs can be executed in reverse to approximate the posterior distribution $p(x|y)$ for any given observation. To compensate for the information loss that inherently occurs in the forward process, an auxiliary latent variable $z \in \mathbb{R}^k$ is introduced, where $k = d - m$ denotes the dimensionality difference between the input and output spaces. The latent variable is sampled from a standard normal distribution $p(z) \sim \mathcal{N}(0, I)$, enabling the model to recover the unresolved components of x that are not deterministic functions of y. An INN architecture is illustrated in Fig. 1.

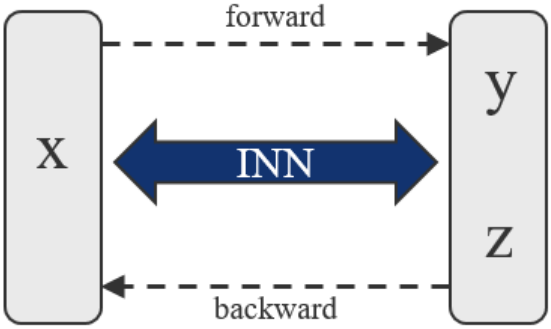

Fig. 1. INN architecture

The inverse problem is reformulated as sampling from an augmented posterior through an invertible function $H(\cdot)$:

$$x = H(y, z; \phi), z \sim p(z) \tag{2}$$

where $H(\cdot)$ is parameterized by INNs with learnable parameters ϕ, while the forward process is defined as:

$$[y, z] = F(x; \phi), H^{-1} = F \tag{3}$$

where the functions $H(\cdot)$ and $F(\cdot)$ share the same weight parameters ϕ and are implemented by a single invertible neural network. The approximated posterior model $p(x|y)$ is representet as:

$$p(x|y) = \frac{p(z)}{\left|\det\left(\frac{\partial H(y,z;\phi)}{\partial [y,z]}\right)\right|} = \frac{p(z)}{|J_x|} \tag{4}$$

where J_x is the Jacobian determinant efficiently computed by affine coupling blocks [17].

The total loss of the proposed INN framework is composed of multiple terms that jointly optimize the forward and inverse mappings between input parameters and output responses. It is formulated as:

$$L_{INN} = \lambda_x L_x + \lambda_y L_y + \lambda_z L_z \tag{5}$$

where λ denotes the weighting factor of each loss component. The output response term L_{y} minimizes the discrepancy between the predicted response $\hat{y}(i)$ and the ground truth $y^*(i)$, ensuring accurate forward prediction:

$$L_y = \sum_i \left(\hat{y}(i) - y^*(i)\right)^2 \tag{6}$$

The latent distribution term L_z penalizes the discrepancy between the joint distribution of network outputs $q(y,z)$, and the product of their marginal distributions $p(y)p(z)$. L_z not only constrains the generated z to follow the prescribed normal distribution $p(z)$ but also enforces statistical independence between y and z, preventing redundant encoding of information. The loss is computed using the Maximum Mean Discrepancy (MMD) and is defined as:

$$L_z = \mathrm{MMD}\left(q(y,z), p(y)p(z)\right) \tag{7}$$

Additionally, the input distribution term L_x minimizes the discrepancy between the distribution of inverse predictions and the true input distribution, ensuring statistical consistency between the generated and empirical inputs. The loss is defined as:

$$L_x = \mathrm{MMD}\left(q(x), p(x)\right) \tag{8}$$

2.3. EXPERIMENT SETUP

The orthogonal cutting experiments are conducted on a specially developed high-precision test bench. The workpiece is mounted on a Kistler force measurement unit (type 9263), which is mechanically coupled to a translational motion stage driven by electromagnetic linear direct drives, while the cutting tool remains stationary. The cutting depth is precisely adjusted using a Keyence laser displacement sensor (LK-H052). During cutting, all force signals generated by the force measurement unit are conditioned by National Instruments charge amplifiers (NI 5015) and subsequently passed through an analogue input module (NI 9215). The digitized signals are continuously sampled and logged in LabVIEW on a PC, where they are further processed for analysis of cutting and thrust force components. The experiment setup is shown in Figure 2 (right).

To ensure a reliable validation of the proposed INN model, the cutting tool, workpiece and cutting conditions in the orthogonal cutting experiments were aligned with those used in the numerical simulations for dataset generation by Reeber et al. [15]. Based on the material

specifications provided in his study, tungsten carbide was selected as the tool material, while AISI 1045 steel was chosen as the workpiece material. An insert from SANDVIK COROMANT was used and subsequently machined on a precision grinding machine at the institute to obtain the required tool geometry (see Table 2). To ensure the manufacturing accuracy of the cutting tool, the rake angle and relief angle were measured using a Keyence digital microscope, as illustrated in Figure 2 (left). The measured nose radius was 20±3 μm. The workpiece was prepared with dimensions of 110 mm × 4 mm × 50 mm and its material composition is listed in Table 3 [18]. The cutting parameters adopted in the orthogonal cutting experiments are presented in Table 4.

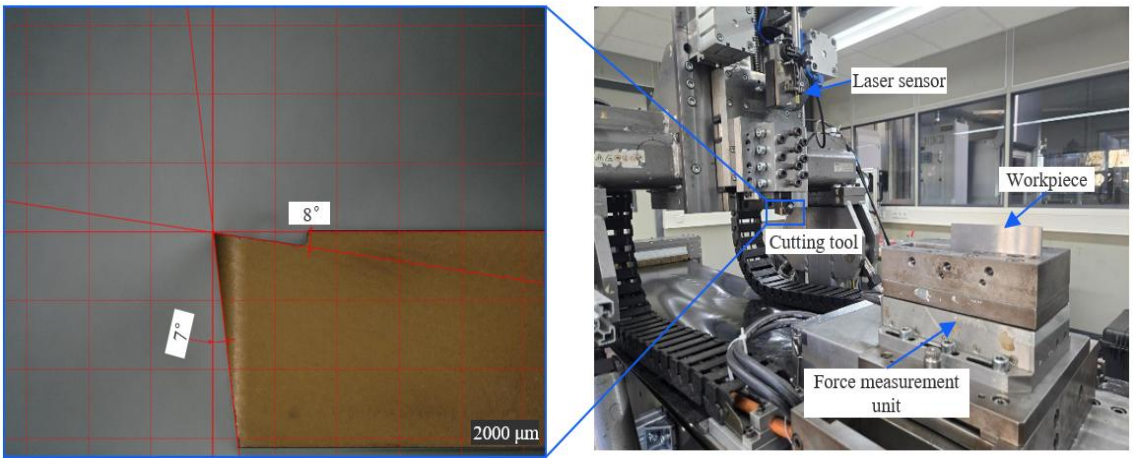

Fig. 2. Experiment setup for orthogonal cutting tests

Table 2. Geometry of the cutting tool

Properties	Rake angle γ [°]	Clearance angle α [°]	Nose radius R [μm]
Value	8	7	20

Table 3. Material composition of AISI 1045

Element	C	Si	Mn	P	S	Cr	Mo	Ni	Al	Cu
Content	0.431	0.233	0.653	0.011	0.024	0.124	0.005	0.018	0.029	0.029

Table 4. Cutting parameters of the experiment

Cutting speed v_c [m/min]	Undeformed chip thickness f [mm]	Width of cutting a_w [mm]
100	0.1	4

3. RESULTS

Figure 3 shows the evaluation of an INN Framework in the inverse directions. In the inverse process, the model generated one set of J-C parameters for each pair of cutting forces in the test dataset. Among the five parameters, the best reconstruction accuracy was achieved for parameter A, with a mean absolute percentage errors (MAPE) below 18% and a

coefficients of determination (R^2) value exceeding 0.7. The parameters B and m were reconstructed with moderate accuracy, yielding MAPE values below 30% and R^2 values higher than 0.4, while parameter n showed a low reconstruction accuracy with an R^2 value around 0.35. Notably, the parameter C appears to be essentially unreconstructable, as indicated by an R^2 value close to zero and a MAPE of approximately 42%. These results indicate that, within our dataset, the cutting forces exhibit high sensitivity to the yield stress constant A, while showing almost no sensitivity to the strain-rate sensitivity coefficient C. This observation is consistent with the findings concluded by Reeber et al. [15].

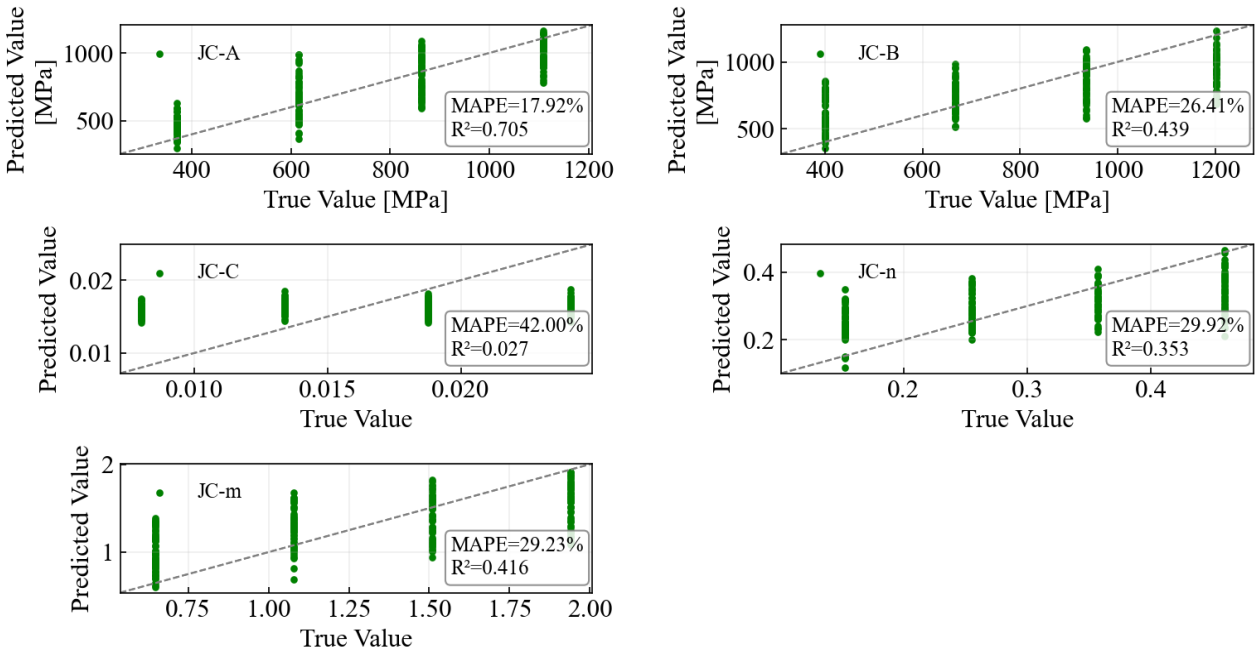

Fig. 3. Evaluation results of the INN model in the inverse directions

In the forward directions, the J-C parameters in the test set were used as input to predict the cutting forces F_c and thrust forces F_t. As shown in Fig. 4, the predicted cutting forces and thrust forces exhibit a strong linear correlation with the true values, with R^2 of 0.951 for F_c and R^2 of 0.966 for F_t.

The MAPE were both below 5% indicating that the INN can accurately capture the nonlinear mapping between J-C parameters and cutting responses. Benefiting from this reliable forward mapping, INN forward model can also replace computationally expensive FE simulations and thereby accelerate the 2D orthogonal cutting analysis.

To verify whether the generated J-C parameters remain physically consistent, each set of generated parameters in inverse process was re-substituted into the forward network to predict the corresponding cutting forces. As shown in Fig. 5, the predicted forces exhibit excellent agreement with their ground truth, resulting a MAPE of 5.93% and an R^2 of 0.931 for F_c, while yielding a MAPE of 3.38% and an R^2 of 0.978 for F_t. Furthermore, it obviously indicates that the generated J-C parameter sets are even more consistent with the thrust force than the cutting force.

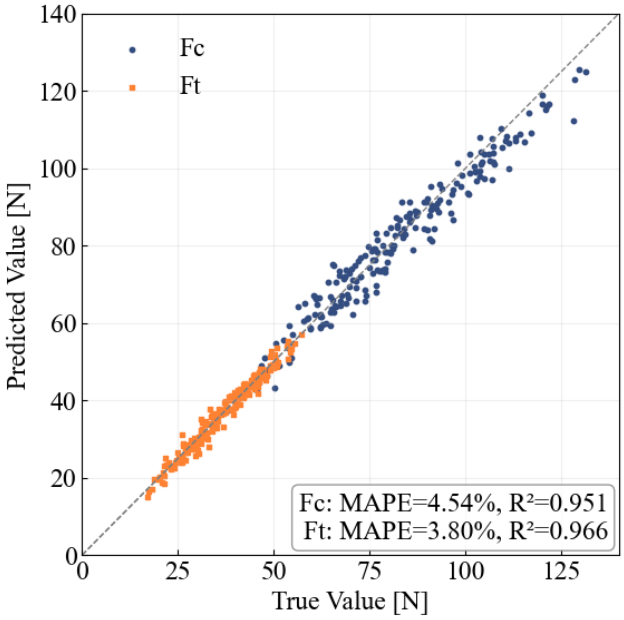

Fig. 4. Evaluation results of the INN model in the forward directions

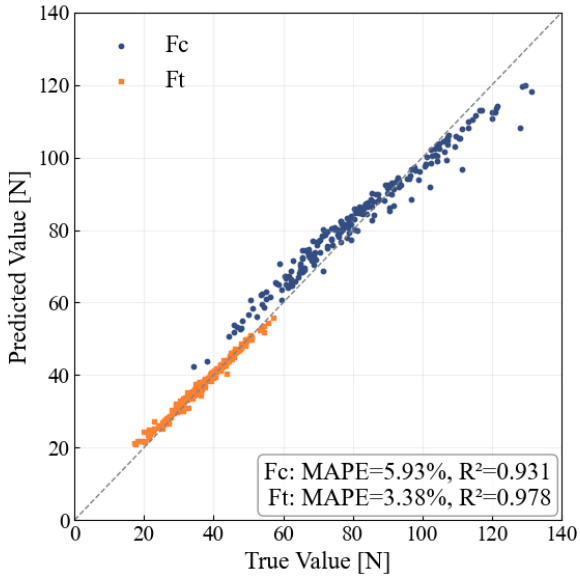

Fig. 5. Evaluation results of the generated J-C parameters using forward network

To assess the stability and robustness of the model, multiple samples were inverse generated under identical input conditions. For a given input instance ($F_c = 113.201$ N and $F_t = 42.37$N), the latent variable z was randomly drawn 1000 times from the standard normal distribution to generate 1000 samples and 10 random samples are listed in Table 5. The resulting J-C parameter distributions are illustrated in Fig. 6. The analysis reveals several insights. First, consistent with the previous observations, the model fails to recover meaningful information for the strain rate sensitivity C, resulting in a MAPE exceeding 100%. Notably, however, the incorrectly reconstructed parameter C still follow a Gaussian-like distribution. This suggests that the model identifies a statistically coherent, yet physically

incorrect surrogate distribution for C, which fits the forward force response despite deviating from the true material behaviour.

Finally, in order to validate the feasibility and physical consistency of the model in real experimental scenarios, an INN-based validation framework that incorporates real orthogonal cutting data was established. In this framework, the cutting force and thrust force measured in the experiments are first used as inputs of the backward direction of the INN to generate the corresponding J-C parameters. These generated parameters are then fed into the forward direction of the INN to predict the cutting force and thrust force, enabling a fast and simulation-free evaluation of the cutting response. The complete framework is illustrated in Fig. 7.

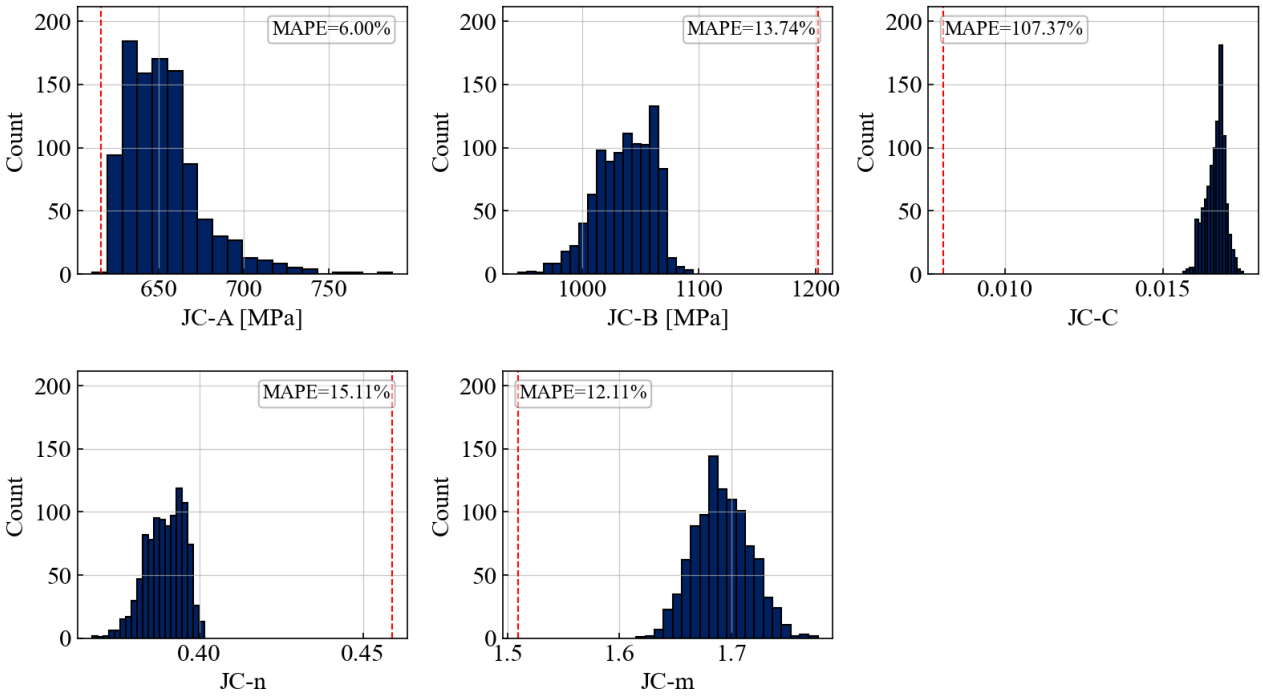

Fig. 6. Sampled J-C parameter distribution for given $F_c = 113.201$ N and $F_t = 42.37$ N. The dashed red line denotes the ground truth

The results of the orthogonal cutting experiments are presented in Figure 8. It should be noted that the y-axis (force) has been scaled according to the workpiece thickness used in the simulations, ensuring that the experimentally measured forces are comparable to the simulated values under consistent geometric conditions. Additionally, the measured force signals were processed using a moving-average filter with a window length of 100 to suppress high-frequency noise and enhance signal clarity.

The J-C parameters generated by the model are listed in Table 6, while the resulting force predictions are depicted as dashed lines in the Figure 8 for comparison with the measured forces in the orthogonal cutting test. The experimental results demonstrate that the employed INN model can also generate physically plausible J-C parameters based on the experimentally measured cutting forces.

Table 5. Generated J-C parameters (10 of 1000 samples) and their ground truth

	A [MPa]	*B* [MPa]	*C*	*n*	*m*
Ground Truth	615.8	1201.86	0.00804	0.459	1.5092
1	656.7365	1050.745	0.016708	0.3894	1.6897
2	654.873	1042.1639	0.016838	0.3925	1.6697
3	734.5027	977.2428	0.016518	0.3906	1.6941
4	649.071	1055.3765	0.016546	0.3966	1.6809
5	673.2345	1000.4816	0.016844	0.3857	1.6829
6	671.3294	1030.0988	0.016151	0.3878	1.6785
7	630.3694	1063.833	0.017021	0.3936	1.66
8	639.1069	1049.4886	0.016773	0.3973	1.6826
9	649.3984	1057.8099	0.016744	0.3937	1.686
10	638.21	1063.5071	0.016853	0.3941	1.6856

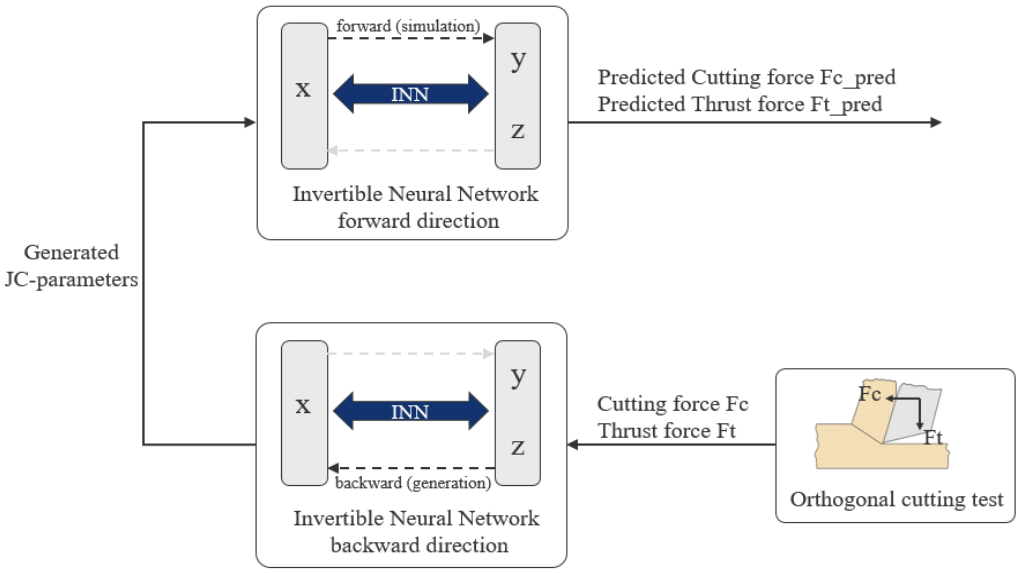

Fig. 7. Framework of the INN-Based J-C parameter inverse identification with experimental validation process

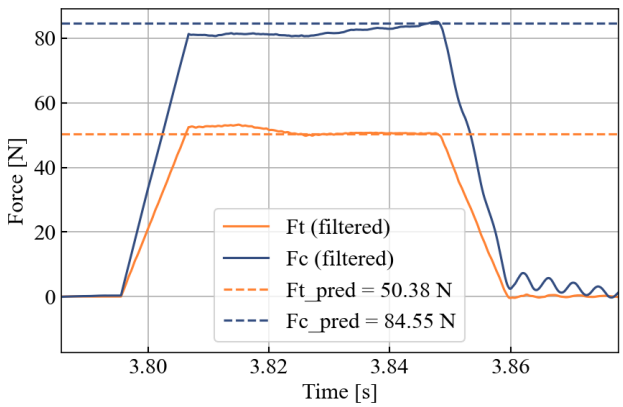

Fig. 8. Comparisons of cutting force and thrust force between model prediction and orthogonal cutting experiment

Table 6. Generated JC-parameters according to cutting and thrust force from orthogonal cutting experiment

A [MPa]	*B* [MPa]	*C*	*n*	*m*
1153.7595	790.4557	0.016098	0.1208	1.2792

4. CONCLUSION

This work presents a data-driven inverse identification framework utilizing an INN to determine J-C parameters from cutting force responses based on AISI 1045. The proposed INN successfully learns a bidirectional mapping between J-C parameters and cutting forces and captures the inherent non-uniqueness in this ill-posed inverse problem. The model not only achieves high forward prediction accuracy for cutting and thrust forces but also enables efficient inverse prediction of multiple J-C parameter candidates, most of which are physically meaningful. Furthermore, the real orthogonal cutting experiments confirm that the generated parameters remain physically plausible when applied to actual cutting conditions.

Despite the promising results, a notable limitation remains. The strain rate sensitivity C cannot yet be reliably reconstructed from the available force data, suggesting that the cutting forces alone do not sufficiently constrain this parameter. To address this limitation and further improve the fidelity of J-C parameter estimation, in the future work, we will expand the dataset to include a richer set of cutting related features, incorporating not only cutting forces but also chip thickness, cutting-zone temperature, and other physically meaningful features. In addition, alternative generative models such as Variational Autoencoder, Generative Adversarial Network will be explored to improve model robustness and posterior expressiveness.

REFERENCES

[1] KUMAR REDDY SIRIGIRI V., YADAV GUDIGA V., SHANKAR GATTU U., SUNEESH G., MOHAN BUDDARAJU K, 2022, *A Review on Johnson Cook Material Model*, Mater Today Proc., 62, 3450–6, https://doi.org/10.1016/j.matpr.2022.04.279.

[2] GRZESIK W., NIESLONY P., LASKOWSKI P., 2017, *Determination of Material Constitutive Laws for Inconel 718 Superalloy Under Different Strain Rates and Working Temperatures*, J. Mater. Eng. Perform., 26, 5705–14, https://doi.org/10.1007/s11665-017-3017-8.

[3] YIN W., LIU Y., HE X., TIAN Z., 2024, *Parametric Analysis and Improvement of the Johnson-Cook Model for a TC4 Titanium Alloy*, Metals, 14, 1199, https://doi.org/10.3390/met14111199.

[4] AGHDAMI A.M., DAVOODI B., 2020, *An Inverse Analysis to Identify the Johnson-Cook Constitutive Model Parameters for Cold Wire Drawing Process*, Mech. Ind., 21, 527, https://doi.org/10.1051/meca/2020070.

[5] KLOCKE F., LUNG D., BUCHKREMER S., 2013, *Inverse Identification of the Constitutive Equation of Inconel 718 and AISI 1045 from FE Machining Simulations*, Procedia CIRP, 8, 212–7, https://doi.org/10.1016/j.procir.2013.06.091.

[6] BÄKER M., 2015, *A New Method to Determine Material Parameters from Machining Simulations Using Inverse Identification*, Procedia CIRP, 31, 399–404, https://doi.org/10.1016/j.procir.2015.04.090.

[7] JIANG X., DING J., WANG C., SHIJU E., HONG L., YAO W., WANG H., ZHOU C., YU W., 2024, *Parameter Identification of Johnson–Cook Constitutive Model Based on Genetic Algorithm and Simulation Analysis for 304 Stainless Steel*, Sci. Rep., 14, 21221, https://doi.org/10.1038/s41598-024-71671-1.

[8] TITU N.A., BAUCUM M., NO T., TROTSKY M., KARANDIKAR J., SCHMITZ T.L., KHOJANDI A., 2021, *Estimating Johnson-Cook Material Parameters Using Neural Networks*, Procedia Manuf., 53, 680–9, https://doi.org/10.1016/j.promfg.2021.06.082.

[9] DUFF M.A.G., CAMPBELL N.D.F., EHRHARDT M.J., 2024, *Regularising Inverse Problems with Generative Machine Learning Models*, J. Math. Imaging. Vis., 66, 37–56, https://doi.org/10.1007/s10851-023-01162-x.
[10] KUMAR P., PATRA A., SHIVALEELA E.S., CALIGIURI V., KRAHNE R., DE LUCA A., SRINIVAS T., 2024, *Multi-Solution Inverse Design in Photonics Using Generative Modeling*, J. Opt. Soc. Am. B, 41, A152. https://doi.org/10.1364/JOSAB.502923.
[11] DAN Y., ZHAO Y., LI X., LI S., HU M., HU J., 2020, *Generative adversarial networks (GAN) based efficient sampling of chemical space for inverse design of inorganic materials*, npj Comput. Mater. 6, 84 https://doi.org/10.48550/arXiv.1911.05020.
[12] ARDIZZONE L., KRUSE J., WIRKERT S., RAHNER D., PELLEGRINI E.W., KLESSEN R.S., MAIER-HEIN L., ROTHER C., KÖTHE U., 2019, *Analyzing Inverse Problems with Invertible Neural Networks*, https://doi.org/10.48550/arXiv.1808.04730.
[13] ALTENBACH H., 2015, *Kontinuumsmechanik: Einführung in Die Materialunabhängigen und Materialabhängigen Gleichungen*, Berlin, Heidelberg, Springer Berlin Heidelberg, https://doi.org/10.1007/978-3-662-47070-1.
[14] COURTNEY, THOMAS H., 2005, *Mechanical behavior of materials*, Waveland Pr Inc.
[15] REEBER T., WOLF J., MÖHRING H.-C., 2024, *A Data-Driven Approach for Cutting Force Prediction in FEM Machining Simulations Using Gradient Boosted Machines*, J. Manuf. Mater. Process., 8, 107, https://doi.org/10.3390/jmmp8030107.
[16] JANG T.J., YOO Y.H., KIM J.B., 2019, *Determination of Johnson-Cook Model Parameters Using Optimization Method*, Trans. Korean Soc. Mech. Eng., A, 43, 951–7.
[17] DINH L., SOHL-DICKSTEIN J., BENGIO S., 2017, *Density estimation using Real NVP*, https://doi.org/10.48550/arXiv.1605.08803.
[18] WOLF J., BANDARU N.K., DIENWIEBEL M., MÖHRING H.-C., 2025, *Image Based Detection of Coating Wear on Cutting Tools with Machine Learning*, J. Mach. Eng., 25, 57–67, https://doi.org/10.36897/jme/196725.